



Article

Is There Daily Growth Hysteresis versus Vapor Pressure Deficit in Cherry Fruit?

Matteo Zucchini ¹, Arash Khosravi ¹, Veronica Giorgi ¹, Adriano Mancini ² and Davide Neri ^{1,*}

¹ Department of Agricultural, Food and Environmental Science, Marche Polytechnic University, 60131 Ancona, Italy; m.zucchini@pm.univpm.it (M.Z.); a.khosravi@pm.univpm.it (A.K.); v.giorgi@staff.univpm.it (V.G.)

² Department of Information Engineering, Marche Polytechnic University, 60131 Ancona, Italy; a.mancini@staff.univpm.it

* Correspondence: d.neri@staff.univpm.it

Abstract: The growth of cherry fruit is generally described using a double sigmoid model, divided into four growth stages. Abiotic factors are considered to be significant components in modifying fruit growth, and among these, the vapor pressure deficit (VPD) is deemed the most effective. In this study, we investigated sweet cherry fruit growth through the continuous, hourly monitoring of fruit transversal diameter over two consecutive years (2019 and 2020), from the beginning of the third stage to maturation (fourth stage). Extensometers were used in the field and VPD was calculated from weather data. The fruit growth pattern up to the end of the third stage demonstrated three critical steps during non-rainy days: shrinkage, stabilization and expansion. In the third stage of fruit growth, a partial clockwise hysteresis curve of circadian growth, as a response to VPD, appeared on random days. The pattern of fruit growth during rainy days was not distinctive, but the amount and duration of rain caused a consequent decrease in the VPD and indirectly boosted fruit growth. At the beginning of the fourth stage, the circadian growth changed and the daily transversal diameter vs VPD formed fully clockwise hysteresis curves for most of this stage. Our findings indicate that hysteresis can be employed to evaluate the initial phenological phase of fruit maturation, as a fully clockwise hysteresis curve was observable only in the fourth stage of fruit growth. There are additional opportunities for its use in the management of fruit production, such as in precision fruit farming.

Keywords: sweet cherry; fruit growth; hysteresis; fruit maturation; vapor pressure deficit (VPD)



Citation: Zucchini, M.; Khosravi, A.; Giorgi, V.; Mancini, A.; Neri, D. Is There Daily Growth Hysteresis versus Vapor Pressure Deficit in Cherry Fruit? *Horticulturae* **2021**, *7*, 131. <https://doi.org/10.3390/horticulturae7060131>

Academic Editor: Luigi De Bellis

Received: 29 April 2021

Accepted: 31 May 2021

Published: 3 June 2021

Publisher's Note: MDPI stays neutral with regard to jurisdictional claims in published maps and institutional affiliations.



Copyright: © 2021 by the authors. Licensee MDPI, Basel, Switzerland. This article is an open access article distributed under the terms and conditions of the Creative Commons Attribution (CC BY) license (<https://creativecommons.org/licenses/by/4.0/>).

1. Introduction

Sweet cherry (*Prunus avium* L.) is a non-climacteric fruit. Most cherry cultivars have red skin with colored flesh at maturation, although some cultivars manifest yellow-red skin with cream-colored flesh and colorless juice, thereby extending their coloration from red to purple and cream to pink [1]. The optimal time for evaluating cherry fruit quality characteristics is determined by changes in skin color and the accumulation of glucose and fructose, which coincide with a fast increase in fruit size [2]. In the maturation period, increasing the fruit weight and anthocyanin content follow sigmoid patterns, whereas the lightness (L), redness (a) and yellowness (b) experience a significant linear decrease during the maturation period [2,3]. Sweet cherry fruit growth is described by a double-sigmoidal pattern, divided into four growth stages. During stage one, cell division in the pericarp occurs. In stage two, the weight remains constant and the endocarp hardens through the lignification of its tissue, while the embryo develops. Stage three is characterized by the rapid expansion of the fruit mesocarp and by an increase in weight [4], whereas stage four begins with fruit maturation and finishes with fruit drop. According to research by Gucci et al. [5], Corelli-Grappadelli and Lakso, [6] and Hammami et al. [7], the fruit maturation process is influenced and regulated by endogenous (biotic) factors, such as

genetic differences and fruit load, and exogenous (abiotic) factors, such as water availability and ambient temperature.

Sweet cherry is highly perishable and is greatly affected by orchard management and environmental conditions [8]. Precision farming is a recent management approach which has been applied in order to increase farming output with less input, through the use of digital technology. A main research focus in precision farming consists in monitoring fruit growth as a continuous recording of fruit diameter with sensors. The observation of circadian cycles, applied to fruit growth, has contributed to the gathering of information regarding this phenological stage and has yielded data for the development of precision farming technologies. Monitoring fruit diameter has been carried out in various studies by researchers measuring diurnal changes in the volume of selected fruits, including peaches [9], grapes [10], kiwifruit [11], sweet [12,13] and pears (Morandi et al., 2014) [14]. Cherry fruit growth during stage 2 and early stage 3 of fruit growth revealed diurnal patterns characterized by net losses of fruit volume during the day and net gains during the night; however, during late stage 3 the diurnal pattern disappeared [12]. In addition to this, fruit growth is highly sensitive to water deficits, which decreases the fruit's biomass accumulation and tissue expansion, while reducing cell numbers [15]. According to Manfrini et al. [16], seasonal fruit monitoring gives researchers the opportunity to forecast the fruit load per tree, fruit size and harvesting time, while also leading operators to adopt more accurate thinning and irrigation practices. Regulated deficit irrigation (RDI) is another benefit which can be extracted from fruit growth monitoring and which has been applied in precision agriculture management for the optimization of irrigation water, without a reduction of yield or fruit quality. A common challenge associated with tree-based sensors is the adjustment of their output to physiologically meaningful parameters in a consistent manner [17,18]. The phenomenon of hysteresis has been known for a long time, attracting the attention of many investigators for years. The reason is that hysteresis is ubiquitous [19]. In Ancient Greek, hysteresis means "to lag behind". Brady and Weil [20] defined it as: "A relationship between two variables that changes depending on the sequences or starting point. An example is the relationship between soil water content and water potential, for which different curves describe the relationship when a soil is gaining water or losing it". In other words, when the time argument of an input function is stretched or compressed, the corresponding output function is not stretched in the same way [21,22].

In cherry plants, Oyarzún et al. [23] observed a hysteresis trend in the diurnal path of transpiration vs. leaf water potential, which roughly described a figure-eight pattern. A similar pattern was observed in laboratory studies by Brüggewirth and Knoche [24] when they investigated the cracking susceptibility of the fruit. They measured the total strain of mature cherry exocarp affected by the pressure applied by an elastometer to simulate the internal pressure of fruit during maturation. This pressure is connected with fruit volume variations and depends on plant water flow and hence on the vapor pressure deficit (VPD). Therefore, we hypothesize that VPD could influence fruit growth, along with hysteresis behavior, in the field.

In this study, we examined daily changes in transversal diameter versus VPD in cherries to verify the presence of differing hysteresis curves in different phenological stages of fruits. The objective of this work was to describe the sweet cherry growth by means of an automatic extensometer within a 2-year time frame (2019 and 2020), for about 33 days, from the beginning of the third stage of fruit growth to fruit maturation. The need for this study was justified by the fact that no previous studies had been conducted on sweet cherries to evaluate the hysteresis cycle vs VPD in terms of the diurnal variation of fruit growth.

2. Materials and Methods

2.1. Site Description and Phenology

This study was conducted in the experimental research station and botanical garden of Polytechnic University of Marche, at Gallignano, in Ancona (AN), Italy (43°34'06.2" N 13°25'24.2" E). The station's 20-year-old sweet cherry orchard, cultivar Blaze Star, grafted on MAXMA 14, was used. The trees were planted in 4.5 m × 3.0 m and trained as a vase system, under organic agriculture management, in rainfed conditions and deep silt clay soil. According to the Köppen–Geiger climate classification, Gallignano belongs to the Cfb category, characterized by warm temperatures and a fully humid and warm summer [25]. The flowering in 2019 was from 29 March 29 to 16 April 16, with the peak on 8 April 8; in 2020, it was from 3 April to 20 April, with the peak on 11 April.

2.2. Fruit Growth

2.2.1. Automatic Extensometer

Fruit diameter was measured in both years from the beginning of third stage of fruit growth to fruit maturation, according to weather conditions. In 2019 the growth of fruit 3 was measured from 4 May (26 DAFB) to 4 June (day of the year—DOY 124 to DOY 155). Fruit 1 growth was measured from 4 May (DOY 124) but dropped on 10 May (DOY 130) and it was substituted with another fruit (fruit 2), which was actively growing until 4 June (DOY 155). In 2020, the growth of one cherry fruit (fruit 4) was measured from 23 April (12 DAFB) to 25 May (DOY 114 to DOY 146).

An electronic extensometer (DEX20, manufactured by Dynamax Inc., Huston, TX, USA), capable of measuring the growth of small fruits (0–25 mm), was used. The DEX20 extensometer is a caliper style device with a full-bridge strain gage attached to a flexible arm and with an output signal range of ±5 mV. The millivolt sensor output measured both the diurnal and long-term growth of fruit. Data were recorded using a Campbell scientific CR100X unit at 1-h intervals and sent to our cloud service, based on Amazon Web Services (AWS), twice per day (Figure 1). The measured daily data were normalized using the Min-Max method with the following equation.

$$x' = 0.9 * ((x - x_{\min}) / (x_{\max} - x_{\min})) + 0.05 \quad (1)$$

where x' is the normalized value, x is the value of the existing data, and x_{\min} and x_{\max} are the minimum and maximum values of the data, respectively.

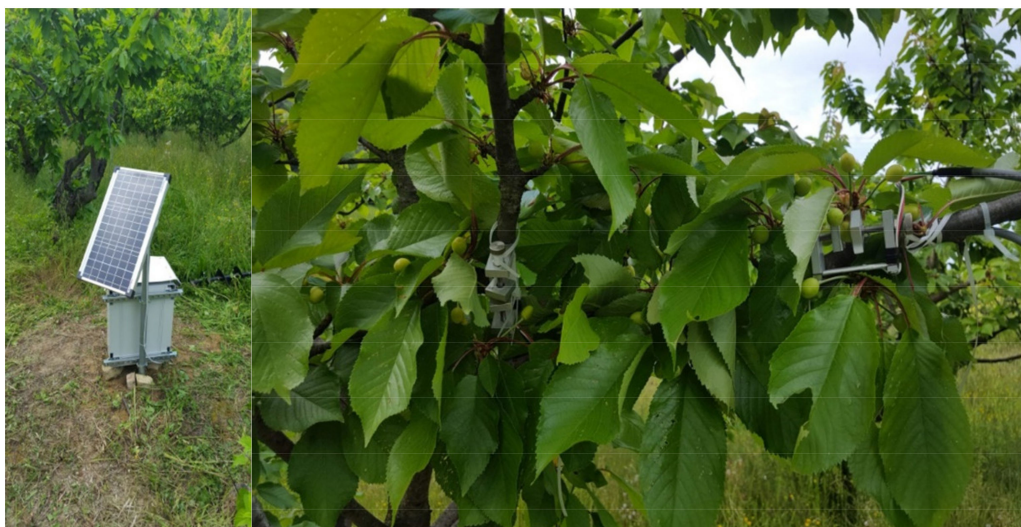


Figure 1. Acquisition system, with a CR100X datalogger (Campbell Scientific Inc., Logan, UT, USA) and an automatic extensometer DEX20 (Dynamax Inc., Huston, TX, USA).

Cherry fruit growth was divided in two time periods according to fruit growth stage. The first period started around the beginning of the third fruit growth stage and finished at the end of this growth stage from DOY 131 to 150 in 2019, and from DOY 114 to 141 in 2020. The second period included the fourth fruit growth stage (i.e., the maturation stage) for a duration of 5 days in both years.

2.2.2. Manual Electronic Caliper

Manual measurements of fruit diameter were performed to represent growth phases in the final part of the double sigmoid curve as a reference for automatic extensometer measurements. One branch per tree from 10 homogeneous trees was randomly selected and on each branch 5 cherry fruits were tagged. The transversal diameter of the tagged fruits was measured from the beginning until the end of the experiment, every 3 to 5 days, with a manual electronic caliper. In the event of fruit abscission, a fruit of comparable size and on the same branch was selected.

2.3. Meteorological Data

Weather data were collected from a Vantage pro2 precision weather station (Davis Instruments Corporation, Hayward, CA, USA) located 500 m away from the cherry orchard. The weather data were automatically transferred to a computer using Vantage pro2, which consisted of weather link software and a data logger. Vapor pressure deficit (VPD) was calculated based on relative humidity (RH) and air temperature (T °C) data, collected from the weather station, with formulas recommended by Monteith and Unsworth [26].

$$\text{VPD} = (1 - (\text{RH}/100)) * \text{SVP} \text{ and } \text{SVP (Pascals)} = 610.7 * 10^{7.5T / (237.3 + T)} \quad (2)$$

where SVP is saturated vapor pressure.

According to the weather station, the sunrise time for all days of the experiment in 2019 and 2020 was set at 6 AM. Our instrument was set to legal Rome time.

2.4. Hysteresis Curve

Hysteresis is non-linear loop-like behavior that does not show affine similarity with respect to time [21,27]. For the description of hysteresis curves, clockwise and anticlockwise loops are referred to. Additionally, the determination of the proper time period for realizing whole-day pictures, as well as seasonal patterns of hysteresis curves, is necessary. Bai et al. [28] suggest dividing daytime hours, as well as growing season, into different periods. Therefore, with consideration of the fruit growth trend over 24 h and the response to VPD, as well as the growth stage of the fruit, the experiments in both years were divided into two periods. In 2019, the first period was from 11 May to 30 May (DOY 131 to 150) and the second period was from 31 May to the end of the experiment, on 4 June (DOY 151 to 155). In 2020, the first period was 23 April to 20 May (DOY 114 to 141) and the second period was from 21 May to 25 May (DOY 142 to 146). Moreover, the graphical representation of daily fruit growth and its fluctuations was reported from 6 AM (approximately the time of sunrise) until 5 AM the next day.

2.5. Data Analysis and Presentation

Data were analyzed using correlation and regression analysis (JMP®, Version 8.0.2.2 SAS Institute Inc., Cary, NC, USA, 1989–2019) and the graphs were drawn using SigmaPlot 11.2 (Systat Software, San Jose, CA, USA).

3. Results

3.1. Fruit Growth Monitoring

The growth season monitored in 2019 was 9 days longer than that in 2020 (Figure 2). Accordingly, the hourly VPD mean for 32 and 33 days was 0.37 ± 0.39 kPa in 2019 and 0.633 ± 0.48 kPa in 2020, respectively.

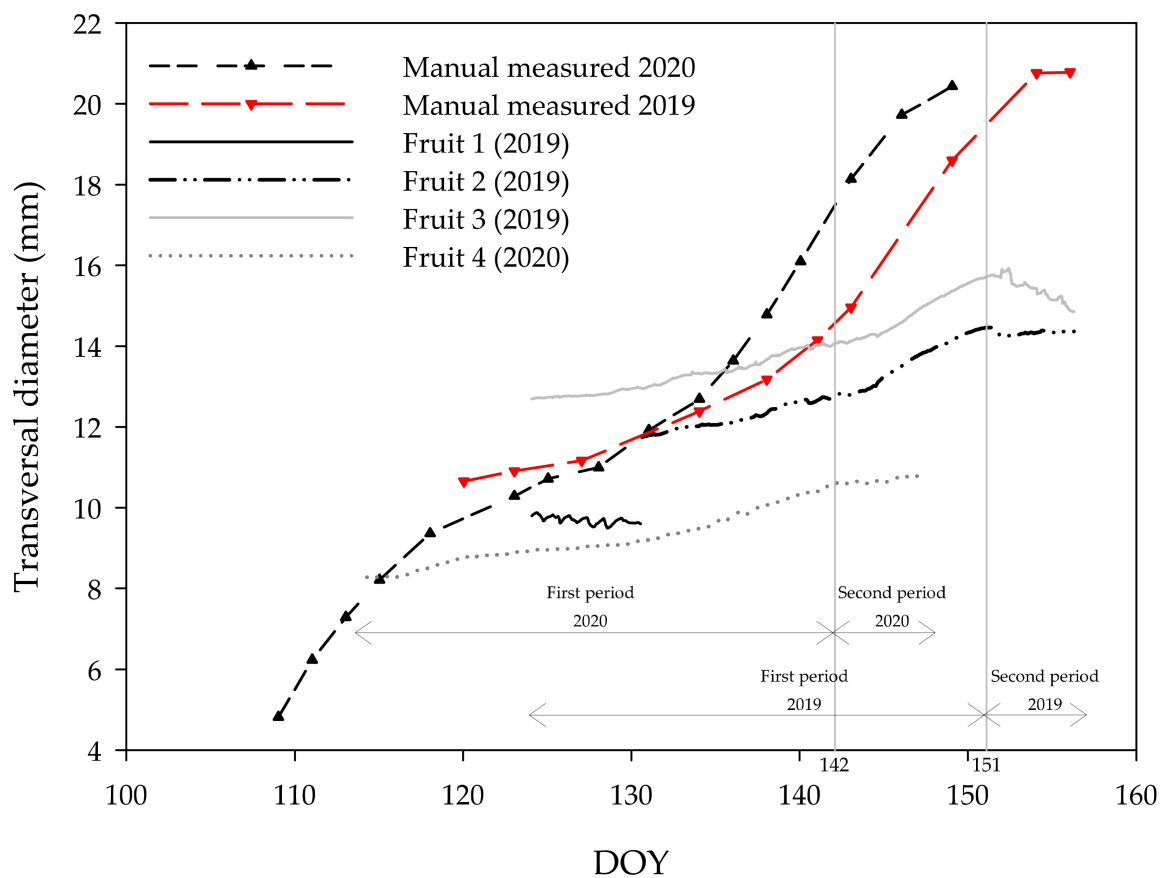


Figure 2. Data interpolation of the 50 labeled fruit in 2019 (manually measured 2019) and 2020 (manually measured 2020); fruit 1 is related to extensometer 1 in 2019; fruit 2 is related to extensimeter 1 in 2019; fruit 3 is related to extensometer 2 in 2019; fruit 4 is related to extensometer 1 in 2020. The first period of the study was from DOY 131 to 150 in 2019 and from DOY 114 to 141 in 2020. The second period of the study was from DOY 151 to 155 in 2019 and from DOY 142 to 146 in 2020.

Comparing manual and automatic diameter measurements, in the first period (third fruit growth stage) of both years of the experiment, the hourly measured transversal diameter by the extensometer showed a similar pattern of growth in all fruits, and the growth was comparable with the trend observed with manual caliper measurements (Figure 2). However, in the second period in both years, the trends of the transversal diameter of the fruits measured using the extensometer were different from those that were manually measured. It could be hypothesized that with the softening of the mesocarp [29], the pressure of extensometer arms acted as a suppressing force. This suppressing force caused the non-similarity of the trends measured using the manual calipers in comparison with those measured using the automatic extensometer. However, the double sigmoidal pattern of growth was maintained in both measuring methods. In addition, the extensometer monitored hourly changes in fruit diameter and the data were reported on the same graph, whereas the manual measurements were interpolated in a continuous line.

In the third fruit growth stage, the most frequent daily pattern of the hourly-measured transversal diameter can be described by three phases (Figure 3) and is comparable to a third-degree polynomial function (66 out of 82 days with a $R^2 \geq 0.75$).

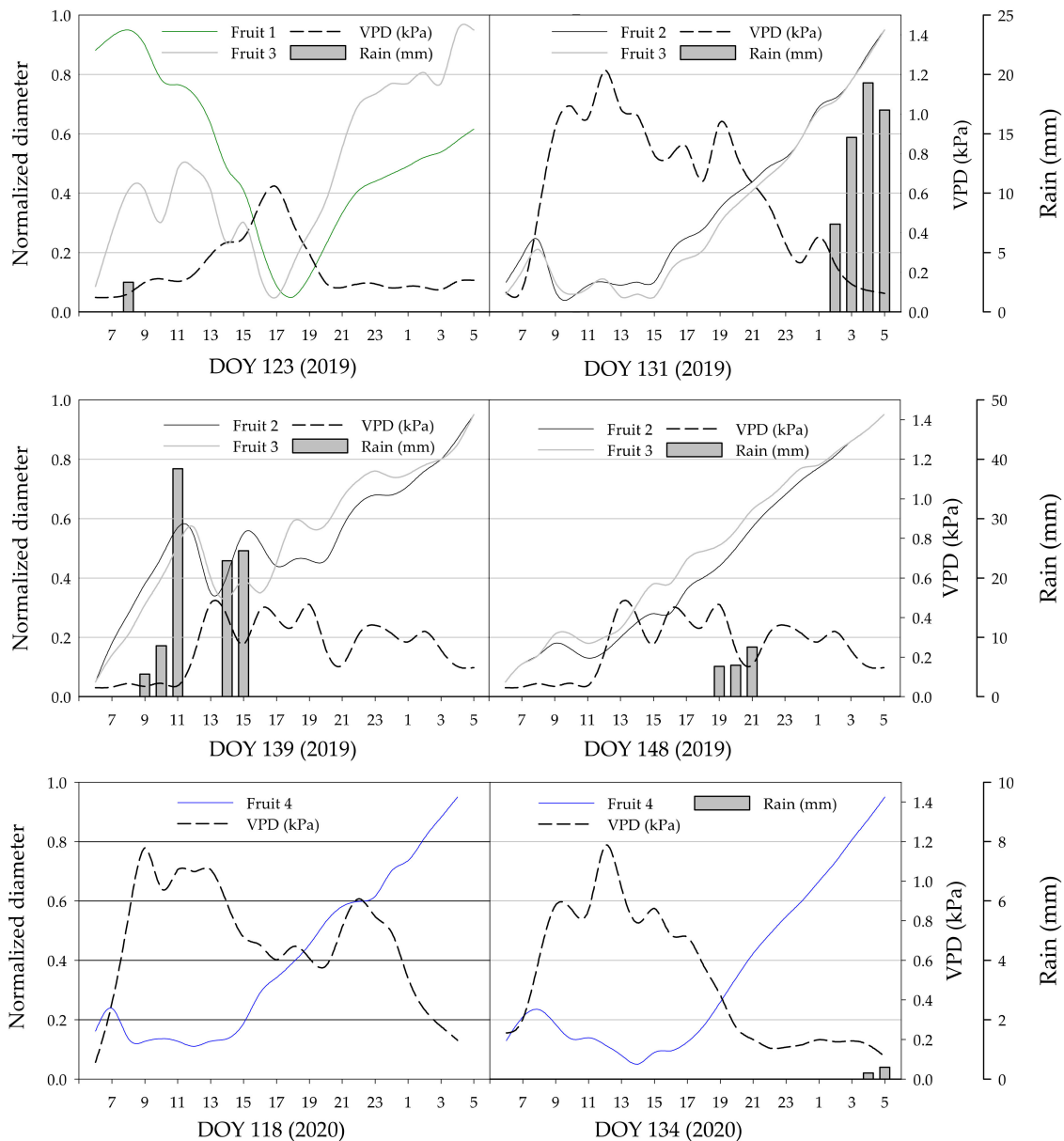


Figure 3. Most representative daily trends of transversal diameter, VPD and rain in the first periods (growth stage 3) in 2019 and 2020. The three-phase daily trend on DOY 118 in 2020 and DOY 131 in 2019; the v-trend of fruit 1 on DOY 123 in 2019; the rain influence on DOY 123, 131 and 139 in 2019 and DOY 141 in 2020.

The first daily phase started at approximately 8.25 a.m. (dev. St. ± 1.38 h) and lasted a few hours. During this phase, the transversal diameter decreased while the VPD increased. The second daily phase revealed substantial stability of the transversal diameter, which overlapped with the maximum VPD values. Then, the results observed in the third phase were opposite to those observed in the first daily phase. This trend started when VPD was at its maximum and lasted until the next day. Fruit diameter increased while VPD decreased.

This daily trend was observable in 58% of the cases in 2019 (14/25 days for fruit 2 and 19/32 days for fruit 3) and 61% in 2020 (20/33 days for fruit 4).

For fruit 1, we observed a decrease in the transversal diameter, followed by a similar increase, with a daily V-shaped trend (Figure 3) until the drop-down of the fruit, which was not able to reach maturity (DOY 130, Figure 2). The daily transversal diameter trend was the opposite of the VPD trend. For fruit 1, when the VPD increased approximately

from sunrise to sunset, negative linear regression versus transversal diameter was detected. Nevertheless, fruits 2, 3 and 4 did not exhibit any kind of regression.

The rain did influence the daily trend of the transversal diameter. When it rained after sunset or in the first hours after sunrise, no response was observed and the transversal diameter followed the three-daily phases (for instance, on DOY 131 of 2019, Figure 3). During the daily phase with increasing VPD, a positive response of transversal diameter to the rain was observed (for instance, DOY 123 and 139 of 2019, Figure 3). However, continuous transversal diameter growth was detected in the days with many hours of rain (for instance, DOY 141 of 2020, Figure 3).

In the second period of both years the fruits monitored using the extensometer did not show a distinct pattern in terms of a daily trend; moreover, the trends of fruits 2, 3 (2019, from DOY 151 to DOY 155) and 4 (2020 from DOY 142 to DOY 146) were different (Figure 2).

For fruit 2, the transversal diameter on DOY 152, 153 and 155 at the end of each day was larger than at the starting point of the same day. However, on DOY 151 and 154 the opposite phenomenon occurred. The diameter decreased by 0.7% during the 5 days of this period (from 14.467 mm to 14.372 mm, Figure 4).

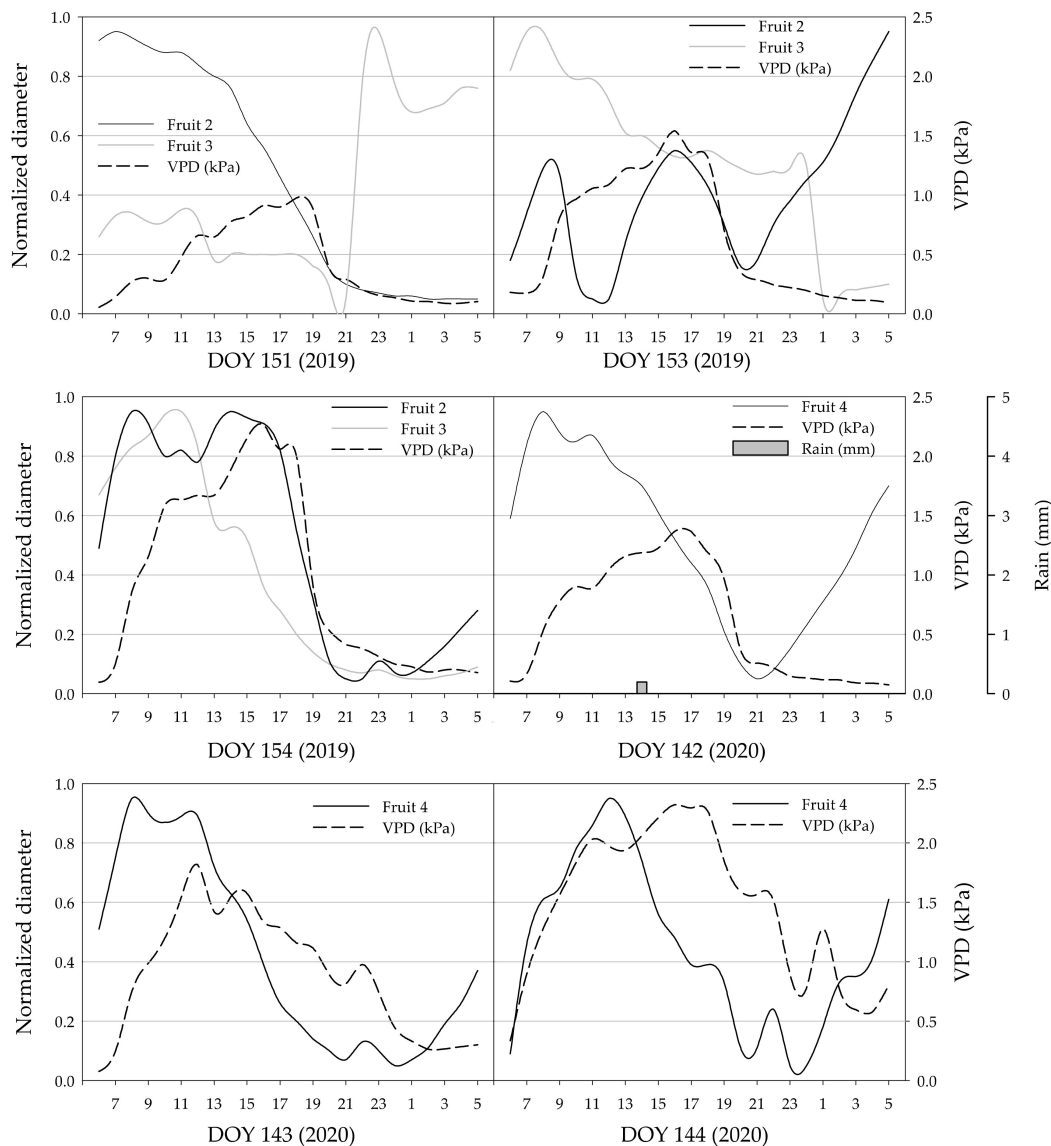


Figure 4. Most representative daily trends of transversal diameter, VPD and rain in the second periods (growth stage 4) in 2019 and 2020.

For fruit 3, on all days except DOY 151, the transversal diameter at the beginning of the day was larger than it was at the end of the same day, decreasing by 5.7% globally (from 15.748 to 14.855 mm, Figure 4).

For fruit 4, on all days except DOY 143, the transversal diameter at the end of the day was larger than at the beginning of the same day, rising by 1.05% (from 10.626 mm to 10.737 mm, Figure 4).

3.2. Analysis of Diameter Growth versus VPD and Hysteresis Curves

In the first periods in 2019 and 2020, the relationship between the VPD and transversal diameter of fruits 2, 3 and 4 did not follow a similar pattern every day. In fact, in some days the trend appeared chaotic, whereas in others it followed a partial clockwise loop (Figure 5, Tables 1–4). Since the observed loops were not representative of the whole day, they can be counted as a partial clockwise hysteresis curve.

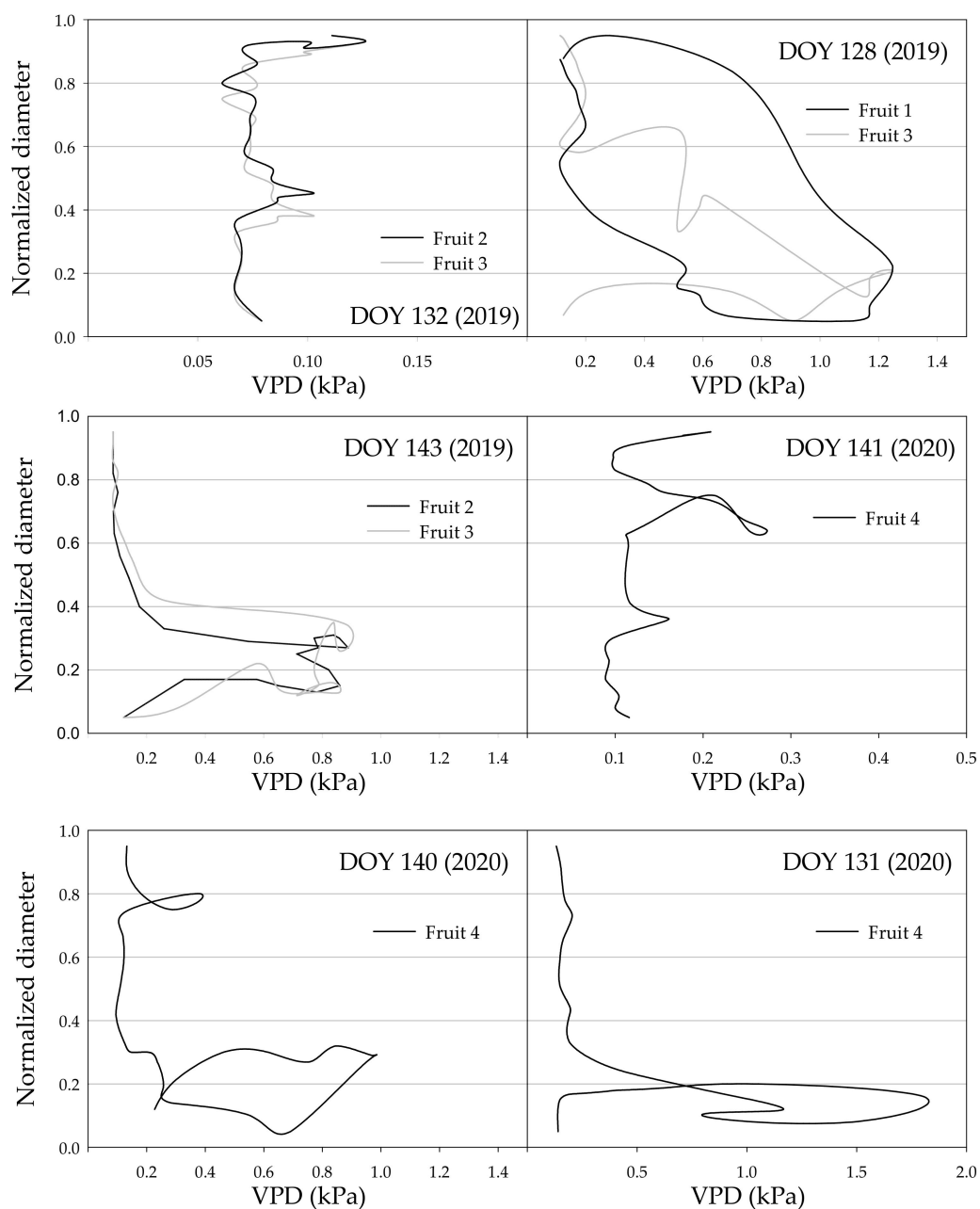


Figure 5. Most representative relations between VPD and transversal diameter in fruit growth stage 3 in 2019 and 2020.

Table 1. Data of daily mean VPD and rainfall for 2019.

DOY	Daily Mean of VPD (kPa)	Rain Fall	Hysteresis Curve		
			Fruit 1	Fruit 2	Fruit 3
124	0.22	Yes	Full		Partial
125	0.17	Yes	Full		Partial
126	0.24	No	Full		Partial
127	0.42	No	Full		No
128	0.47	Yes	Full		Partial
129	0.20	Yes	No		Partial
130	0.50	No			Partial
131	0.60	Yes		No	No
132	0.08	Yes		No	No
133	0.15	Yes		No	No
134	0.19	Yes		Partial	Partial
135	0.19	Yes		Partial	Partial
136	0.25	No		No	No
137	0.32	No		Partial	Partial
138	0.19	Yes		Partial	Partial
139	0.25	Yes		No	No
140	0.50	No		Partial	Partial
141	0.47	No		Partial	Partial
142	0.53	No		Partial	Partial
143	0.45	No		No	No
144	0.50	No		No	Partial
145	0.52	Yes		No	No
146	0.14	Yes		No	No
147	0.18	Yes		No	No
148	0.22	Yes		No	No
149	0.10	Yes		No	No
150	0.13	Yes		No	No
151	0.41	No		Full	Partial
152	0.64	No		No	Full
153	0.63	No		Partial	Full
154	0.96	No		Full	Full
155	0.99	No		Full	Full

Table 2. Data of daily mean VPD and rainfall for 2020.

DOY	Daily Mean of VPD (kPa)	Rain Fall	Hysteresis Curve
114	0.28	No	Partial
115	0.73	No	Partial
116	0.83	No	No
117	0.61	No	No
118	0.67	No	No
119	0.37	Yes	No
120	0.54	Yes	No
121	0.7	No	No
122	0.8	Yes	No
123	0.59	No	No
124	0.38	Yes	Partial
125	0.74	No	Partial
126	1.06	No	No
127	0.26	No	No
128	0.53	Yes	Partial
129	0.96	No	No
130	0.78	No	No
131	0.51	No	Partial
132	0.71	No	No
133	0.7	Yes	No

Table 2. *Cont.*

DOY	Daily Mean of VPD (kPa)	Rain Fall	Hysteresis Curve
134	0.49	Yes	Partial
135	0.39	No	Partial
136	0.88	No	Partial
137	0.41	Yes	No
138	0.34	No	Partial
139	0.31	No	No
140	0.38	Yes	Partial
141	0.15	Yes	No
142	0.6	Yes	Full
143	0.89	No	Full
144	1.47	No	Full
145	0.47	Yes	No
146	1.02	No	Partial

Table 3. Frequency of observations showing hysteresis curves in fruits 2, 3 and 4 in the first period of study. Pearson test was not significant (p -value > 0.05).

Hysteresis Curve	Frequency
No hysteresis	0.573
Partial	0.427
Full	-
Pearson test value	0.204

Table 4. Frequency of the observations showing hysteresis curves in fruits 2, 3 and 4 in the second period of study. Asterisk indicates that Pearson test was significant (p -value < 0.05).

Hysteresis Curve	Frequency
No hysteresis	0.133
Partial	0.200
Full	0.667
Pearson test value	0.0224 *

On the other hand, fruit 1 showed a complete clockwise hysteresis curve (Figure 5) on 5 days out of 6 studied (from DOY 124 to DOY 129). On the last day (DOY 129), no hysteresis could be observed because during the second part of the day the transversal diameter did not increase (Table 3).

In the second period, the VPD increased to 0.74 ± 0.62 kPa (from 0.30 ± 0.62 kPa in the first period) in 2019 and to 0.89 ± 0.63 (from 0.58 ± 0.43 kPa in the first period) in 2020.

With the softening of the mesocarp, the pressure of the arms of the extensometer acted as a suppressing force (Figure 6). Thus, the transversal diameters of the fruits appeared to be decreasing. For this reason, although the curves did not close, we can consider them to exhibit hysteresis.

Thus, in two out of 15 total studied cases (5 days of the second stage for the three fruits) there was no hysteresis, in three out of 15 there was partial hysteresis, and in 10 out of 15 there was full hysteresis (Tables 3 and 4). Full hysteresis delimited a greater area than partial hysteresis (Figures 5 and 7).

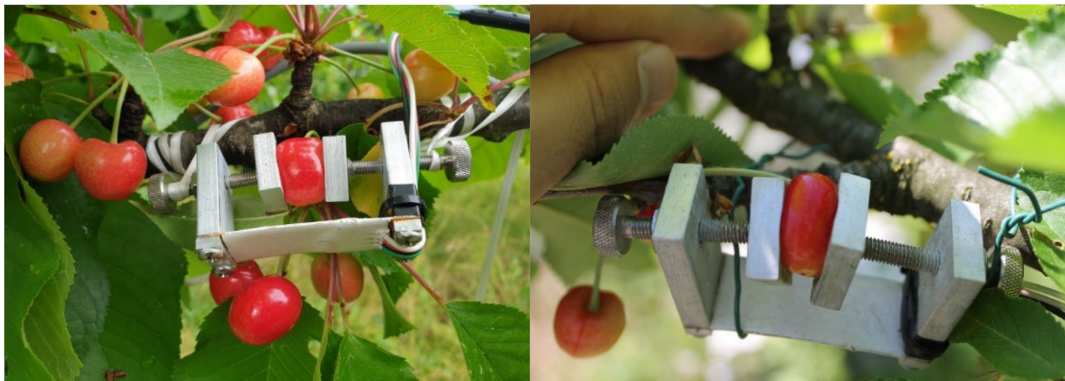


Figure 6. Cherry fruits on 28 May 2019 (DOY 148, left) and 22 May 2020 (DOY 143, right).

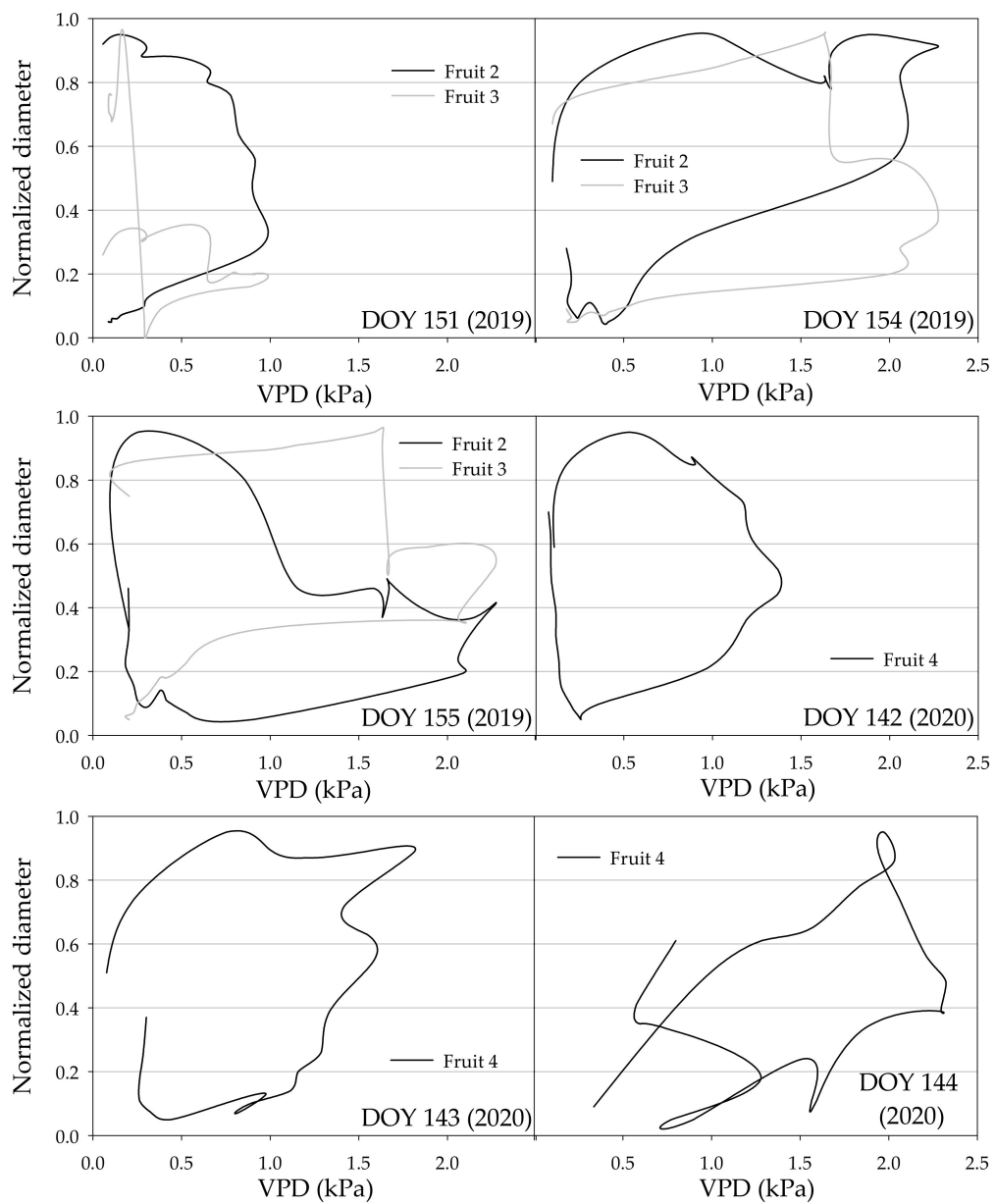


Figure 7. Most representative relations between VPD and transversal diameter in fruit growth stage 4 in 2019 and 2020.

4. Discussion

The results of this study showed that VPD can influence daily fruit growth and even induce full clockwise hysteresis during maturation. It is likely that the maturation date for the cherry fruit can be anticipated if the average VPD is higher, as it was in 2020, when the growth season was shorter than in 2019.

Generally, growing fruits can recover the shrinkage which was recorded in the early morning due to the VPD increase during the afternoon and the night, when the VPD is lower. On the contrary, fruits that are close to drop-down (for example, fruit 1) undergo a size reduction without early recovery, possibly due to the loss of inflow capacity from the tree [12] and related to abscising set formation between the fruit and the pedicel.

Therefore, the difference between growing fruit (fruits 2, 3 and 4) and dropping fruit (fruit 1) was observable when the VPD increased from the sunrise. With daily increases in VPD, fruits 2, 3 and 4 showed a short period of diameter decrease and then a stability phase in terms of diameter. However, in fruit 1, the diameter stability phase was not detectable. On the other hand, all fruits showed strong growth during the VPD decrease from sunset to sunrise.

Rain can change the diameter growth trend during the daylight phase, causing a decrease in VPD and a boost in the fruit diameter, likely related to a water boost, as was found by Correia et al. [8]. This phenomenon depends on the intensity of rain, the rainy hours and the circadian time of the rain.

During the third fruit growth period, the relation between VPD and transversal diameter showed partial hysteresis in the daily phases between sunrise and sunset. From sunset, the transversal diameter grew exponentially as the VPD decreased, defined by a power trend of the curve.

The behavior of fruit 1 was also observable in fruits 2, 3 and 4 during the second period of the study (the maturation stage). In this stage, the mean hourly VPD increased in both years. Brüggewirth et al. [12] demonstrated that transpiration flow in sweet cherry fruit is closely linked to VPD throughout development. The dependence on the VPD increases because the stomata lose their functionality during stage three [30]. During this stage, it can be hypothesized that the xylem inflow equalizes the outgoing transpiration outflow, but in late stage three (around the beginning of second study period) the water uptake from the xylem to the fruit is getting close to zero [12,31,32]. The VPD increase during the day, together with the non-functionality of some stomata, plus the stopping of the xylem conductivity, may have caused the final size decrease observed in the fruits in 2019, and hampered growth in 2020.

In addition, during stage four of fruit development, the softening of the mesocarp increased [29] and the fruit was unable to oppose the pressure of the extensometer arms. In this period, the limited phloem connection may still help recover the water during the night, and thus the daily fruit growth trend realized a full hysteresis curve, in which the return curve did not overlap with the forward curve, nor did it pass close to it. In the case of partial hysteresis, the outward and return curves were very close.

Considering the results for 2019 and 2020, it can be hypothesized that a fully clockwise hysteresis curve is observable only when cherry fruits are fully mature (Tables 3 and 4). Thus, the mature fruit can exhibit large differences in size during the day, depending on VPD [12].

5. Conclusions

In this study, we investigated the continuous transversal diameter growth of sweet cherry fruits in 2019 and 2020, and considered its relationship with VPD. The results showed that on some random days of the third stage of fruit growth, the response of fruit transversal diameter versus VPD demonstrated a partial clockwise hysteresis curve. Only in the fourth stage of fruit growth was fully clockwise hysteresis detectable. Thus, the detection of partial and fully clockwise hysteresis curves can be considered a useful tool

in monitoring the real phenological stages of fruit and can be used as a basis to develop precision farming techniques applied to decision support systems (DSSs).

Author Contributions: Conceptualization, D.N. and A.M.; methodology, M.Z. and A.K.; software, A.M.; investigation, D.N.; data curation, A.M.; writing—original draft preparation, M.Z. and A.K.; writing—review and editing, D.N., V.G., M.Z. and A.K.; supervision, D.N.; project administration, D.N.; funding acquisition, D.N. and A.M. All authors have read and agreed to the published version of the manuscript.

Funding: This research was funded by Polytechnic University of Marche, with “The network of the Botanical Gardens of Ancona PSA 2017-18” project.

Data Availability Statement: All data are available with an email request to the authors.

Conflicts of Interest: The authors declare no conflict of interest.

References

- Iezzoni, A.F. Cherries. In *Temperate Fruit Crop Breeding*; Hancock, J.F., Ed.; Springer: New York, NY, USA, 2008; pp. 151–175.
- Serrano, M.; Guillen, F.; Martinez-Romero, D.; Castillo, S.; Valero, D. Chemical constituents and antioxidant activity of sweet cherry at different ripening stages. *J. Agric. Food Chem.* **2005**, *53*, 2741–2745. [[CrossRef](#)] [[PubMed](#)]
- Gonçalves, B.; Silva, A.P.; Outinho-peria, J.M.; Bacelar, E.; Rosa, E.; Meyer, A.S. Effect of ripeness and postharvest storage on the evolution of colour and anthocyanins in cherries (*Prunus avium* L.). *Food Chem.* **2007**, *103*, 976–984. [[CrossRef](#)]
- Knoche, M.; Peschel, S.; Hinz, M.; Bukovac, M.J. Studies on water transport through the sweet cherry fruit surface: II. Conductance of the cuticle in relation to fruit development. *Planta* **2001**, *213*, 927–936. [[CrossRef](#)]
- Gucci, R.; Lodolini, E.M.; Rapoport, H.F. Water deficit-induced changes in mesocarp cellular processes and the relationship between mesocarp and endocarp during olive fruit development. *Tree Physiol.* **2009**, *29*, 1575–1585. [[CrossRef](#)] [[PubMed](#)]
- Corelli-Grappadelli, L.; Lakso, A.N. Fruit development in deciduous tree crops as affected by physiological factors and environmental conditions (keynote). In Proceedings of the XXVI International Horticultural Congress: Key Processes in the Growth and Cropping of Deciduous Fruit and Nut Trees, Toronto, ON, Canada, 11–17 August 2002; Volume 636, pp. 425–441.
- Hammami, S.B.; Manrique, T.; Rapoport, H.F. Cultivar-based fruit size in olive depends on different tissue and cellular processes throughout growth. *Sci. Hortic.* **2011**, *130*, 445–451. [[CrossRef](#)]
- Correia, S.; Schouten, R.; Silva, A.P.; Gonçalves, B. Sweet cherry fruit cracking mechanisms and prevention strategies: A review. *Sci. Hortic.* **2018**, *240*, 369–377. [[CrossRef](#)]
- Montanaro, G.; Dichio, B.; Xiloyannis, C.; Celano, G. Light influences transpiration and calcium accumulation in fruit of kiwifruit plants (*Actinidia deliciosa* var. *deliciosa*). *Plant Sci.* **2006**, *170*, 520–527. [[CrossRef](#)]
- Greenspan, M.D.; Shackel, K.A.; Matthews, M.A. Developmental changes in the diurnal water budget of the grape berry exposed to water deficits. *Plant Cell Environ.* **1994**, *17*, 811–820. [[CrossRef](#)]
- Li, S.H.; Génard, M.; Bussi, C.; Lescourret, F.; Laurent, R.; Besset, J.; Habib, R. Preliminary study on transpiration of peaches and nectarines. *Gartenbauwissenschaft* **2002**, *67*, 39–43.
- Brüggenwirth, M.; Winkler, A.; Knoche, M. Xylem, phloem, and transpiration flows in developing sweet cherry fruit. *Trees* **2016**, *30*, 1822–1830. [[CrossRef](#)]
- Mancini, A.; Zucchini, M.; Poverigiani, S.; Marcheggiani, E.; Casavecchia, S.; Neri, D. Cherry Fruit Growth: Monitoring and ‘Tweeeting’. *Acta Hortic.* **2021**, in press.
- Morandi, B.; Losciale, P.; Manfrini, L.; Zibordi, M.; Anconelli, S.; Galli, F.; Pierpaoli, E.; Grappadelli, L.C. Increasing water stress negatively affects pear fruit growth by reducing first its xylem and then its phloem inflow. *J. Plant Physiol.* **2014**, *171*, 1500–1509. [[CrossRef](#)]
- Tardieu, F.; Granier, C.; Muller, B. Water deficit and growth. Co-ordinating processes without an orchestrator? *Curr. Opin. Plant Biol.* **2011**, *14*, 283–289. [[CrossRef](#)] [[PubMed](#)]
- Manfrini, L.; Pierpaoli, E.; Taylor, J.A.; Morandi, B.; Losciale, P.; Zibordi, M.; Corelli-Grappadelli, L.; Bastias, R.M. Precision fruit growing: How to collect and interpret data on seasonal variation in apple orchards. In Proceedings of the XXVIII International Horticultural Congress on Science and Horticulture for People (IHC2010): International Symposium on Plant, Lisbon, Portugal, 22–27 August 2010; Volume 932, pp. 461–469.
- Fernández, J. Plant-based methods for irrigation scheduling of woody crops. *Horticulturae* **2017**, *3*, 35. [[CrossRef](#)]
- Jones, H.G. Monitoring plant and soil water status: Established and novel methods revisited and their relevance to studies of drought tolerance. *J. Exp. Bot.* **2006**, *58*, 119–130. [[CrossRef](#)] [[PubMed](#)]
- Mayergoyz, I.D. *Mathematical Models of Hysteresis and Their Applications: Second Edition (Electromagnetism)*; Academic Press: Cambridge, MA, USA, 2003; ISBN 978-0-12-480873-7.
- Brady, N.C.; Weil, R.R. *The Nature and Properties of Soils*, 13th ed.; Prentice Hall: Upper Saddle River, NJ, USA, 2002; p. 922.
- O’Kane, J.P. Hysteresis in hydrology. *Acta Geophys. Pol.* **2005**, *53*, 373–383.

22. Zhang, Q.; Manzoni, S.; Katul, G.; Porporato, A.; Yang, D. The hysteretic evapotranspiration—Vapor pressure deficit relation. *J. Geophys. Res. Biogeosci.* **2014**, *119*, 125–140. [[CrossRef](#)]
23. Oyarzún, R.; Stockle, C.; Whiting, M. Hydraulic conductance determination and its components in field grown mature sweet cherry trees. *Acta Hortic.* **2008**, *795*, 691–694. [[CrossRef](#)]
24. Brüggewirth, M.; Knoche, M. Mechanical properties of skins of sweet cherry fruit of differing susceptibilities to cracking. *J. Am. Soc. Hortic. Sci.* **2016**, *141*, 162–168. [[CrossRef](#)]
25. Kottke, M.; Grieser, J.; Beck, C.; Rudolf, B.; Rubel, F. World map of Köppen-Geiger climate classification updated. *Meteorol. Z.* **2006**, *15*, 259–263. [[CrossRef](#)]
26. Monteith, J.; Unsworth, M. *Principles of Environmental Physics: Plants, Animals, and the Atmosphere*; Academic Press: Cambridge, MA, USA, 2013.
27. Phillips, J.D. Sources of nonlinearity and complexity in geomorphic systems. *Prog. Phys. Geogr.* **2003**, *27*, 1–23. [[CrossRef](#)]
28. Bai, Y.; Li, X.; Liu, S.; Wang, P. Modelling diurnal and seasonal hysteresis phenomena of canopy conductance in an oasis forest ecosystem. *Agric. Forest Meteorol.* **2017**, *246*, 98–110. [[CrossRef](#)]
29. Schumann, C.; Schlegel, H.J.; Grimm, E.; Knoche, M. Water potential and its components in developing sweet cherry. *J. Am. Soc. Hortic. Sci.* **2014**, *139*, 349–355. [[CrossRef](#)]
30. Peschel, S.; Beyer, M.; Knoche, M. Surface characteristics of sweet cherry fruit: Stomata-number, distribution, functionality and surface wetting. *Sci. Hortic.* **2003**, *97*, 265–278. [[CrossRef](#)]
31. Grimm, E.; Pflugfelder, D.; van Dusschoten, D.; Winkler, A.; Knoche, M. Physical rupture of the xylem in developing sweet cherry fruit causes progressive decline in xylem sap inflow rate. *Planta* **2017**, *246*, 659–672. [[CrossRef](#)]
32. Winkler, A.; Brüggewirth, M.; Ngo, N.S.; Knoche, M. Fruit apoplast tension draws xylem water into mature sweet cherries. *Sci. Hortic.* **2016**, *209*, 270–278. [[CrossRef](#)]